COMPUTATIONAL FLUID DYNAMIC SIMULATION OF SWIRL FLOW IN HEXAGONAL ROD BUNDLE GEOMETRY BY SPLIT MIXING VANE GRID SPACERS

by

Mohammad NAZIFIFARD [*]

Department of Energy Systems Engineering, Energy Research Institute,
University of Kashan, Kashan, Iran

Original scientific paper
https://doi.org/10.2298/TSCI171006076N

Heat transfer and pressure drop are numerically investigated for turbulent flows through a hexagonal fuel rod bundle. For the purpose of numerical analysis, the geometric and boundary conditions were taken from the VVER-1000. Since VVER-1000 does not have mixing vane on the grid spacer of the fuel assembly, split mixing vane is designed to boost turbulent flow and heat transfer in the rod bundle subchannels. The computational domain including two grid spacers extend from $100 \times D_h$ upstream of the first grid spacer to $250 \times D_h$ downstream of the second grid spacer. The steady-state form of the RANS, mass, energy and turbulence equations was discretized and solved using ANSYS-CFX. The standard k-ε model is employed to simulate turbulence. The results show a considerable increase in the average heat transfer to $\sim 10 \times D_h$ downstream of the grid spacer using the mixing vane on the grid spacer of VVER type reactor. As expected, the pressure loss through the grid spacer also increased slightly with the mixing vanes.

Key words: *pressurised water reactor, VVER 1000, heat transfer enhancement, CFD, turbulence model, mixing vane*

Introduction

In the pressurized water reactor (PWR) work, the coolant is in the forced and turbulent convection. The average heat transfer coefficient in force convection is generally governed by those factors representing turbulence and operating conditions. Generally, a larger and more uniform single phase local heat transfer coefficient yields increased performance, and prevents the nuclear fuel rods from potential damage by increased temperature. There are different methods to enhance the local heat transfer rate in the PWR core. The mixing vanes grid spacers are one of the most widely used groups of heat transfer enhancement tools to boost turbulent flow and heat transfer in the PWR fuel subchannels. The grid spacers and mixing vanes have since 1970's undergone gradual development in order to improve their performance [1-13]. Preliminary experimental analysis of PWR grid spacer was undertaken by Rehme [1-3] that resulted in correlations for several grid spacers without mixing vanes. Also, in the field of experimental study related to heat transfer, several researcher [4-7] showed locally enhanced heat transfer downstream of the grid spacer in the PWR rod bundles. Schikorr *et al.* [14] improved Rehme's correlation include grid spacers with mixing devices based on new pressure drop measurements. Morovere, recent studies [15-31] have reported that the mixing vanes cause cross and

[*] Author's e-mail: nazifi@kashanu.ac.ir

swirl flows amongst and within the subchannels enhancing heat transfer in the vicinity of the grid spacer. However, the main role of the mixing vane in the rod bundle is the enhancement of critical heat flux (CHF) and departure from nucleate boiling (DNB) which could contribute to the improvement of reactor safety [12, 27]. A study by Song *et al.* [12] showed the standard split vane could enhance the CHF by up to 14.5% when compared with the grid spacer without a mixing vane for PWR. Albeit the DNB phenomenon for nuclear rod bundle is analyzed by CFD under a two-phase flow condition, the distribution of fluid enthalpy and the Nusselt number under a single phase flow will determine the initial conditions and important information regarding the two-phase flow structure [10, 15]. However, a major problem with the mixing vane is the additional pressure drop which could increase the reactor pumping costs. The pressure drop depends on the grid spacer and mixing vane design. Numerous studies have showed [13, 28, 30, 31] that the addition of mixing vane on the grid spacer generates more anisotropic axial swirling pattern compared against the standard grid spacer. Nematollahi and Nazifi [13] showed that the standard split mixing vane is expected to significantly enhance the overall heat transfer of a nuclear fuel assembly by 9.82% with a reasonable increase in the pumping cost. Toth and Aszodi [16] emphasized that the grid spacer has an important bearing on the cross-flows, axial velocity and outlet temperature distribution in subchannels. Toth and Aszodi [17] in another CFD study improved the full length fuel bundle and 60° segment model for a VVER-440 fuel assembly. They proved that the coolant mixing is more intensive in the fuel assembly head than in the rod bundle. The CFD analysis revealed that the outflow from the central tube influences strongly the in-core temperature measurement. Therefore, this effect has to be taken into account in VVER assembly head calculations. Hutli *et al.* [26] investigated experimentally the increase of mixing phenomenon in a coolant flow in order to improve the heat transfer, the economical operation and the structural integrity of VVER-440 using PIV and PLIF techniques. They obtained detailed information on the velocity, turbulence and temperature distribution for parallel turbulent flows through sub-channels of a hexagonal VVER-type rod bundle.

The literature survey ended up no data to be found on the presence of a mixing vane on the grid spacer of VVER 1000. In addition, there is a scarcity of work done for design of a mixing vane for the VVER type reactor. In this study, split mixing vanes are designed for VVER-1000. A CFD analysis is performed to analyse the heat transfer and additional pressure drop on the mixing vane.

Numerical simulation

For the purpose of simulations, the geometry and boundary conditions were extracted from the VVER-1000 core. The VVER-1000 is a Russian designed PWR with a hexagonal fuel assembly geometry. In western PWR, the mixing vanes are attached to the grid spacers of rod bundle to enhance thermal performance by promoting the turbulence level, increasing inter-subchannel mixing, and inducing swirl flows. Since VVER-1000 does not have mixing vane on the grid spacer of the fuel assembly, mixing vane is designed to boost turbulent flow and heat transfer in the rod bundle subchannels. The mixing vane in this study is similar with the standard split vane of ordinary PWR except that it is customized for VVER-1000. The mixing vanes may as well be incorporated in the actual rod bundle for VVER-1000. The clockwise swirling arrangement is applied for the mixing vanes. The computational domain consists of 610 mm long models containing 7 fuel rods of VVER-1000 rod bundle with an outer diameter of 9.1 mm and the rod pitch of 12.3 mm, fig. 1. The grid spacer was modeled considering its wall thickness. The cross-sectional area of the model and the grid spacer are depicted in fig. 2. The unstructured meshes were applied in the center of channels, and fine layers close to the walls. Cross-sectional

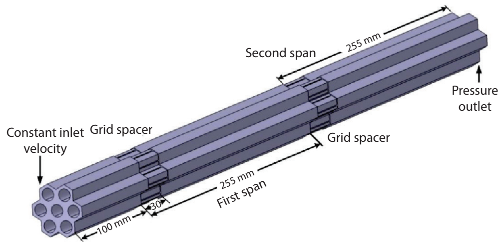

Figure 1. Computational flow domain

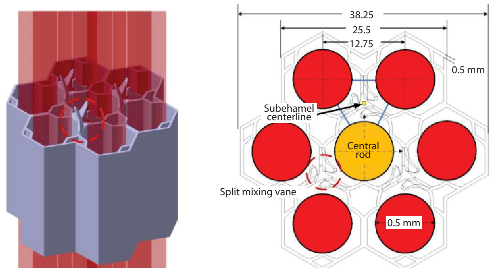

Figure 2. Schematic figures of mixing vane on grid spacer

grid distribution is depicted in fig. 3. Unstructured meshes in the center of channels region and fine layers close to the walls were applied. In order to check on the influence of the mesh resolution on the results and to minimize the numerical influences introduced by the size of meshes and their distributions, comprehensive mesh sensitivity study was performed pursuant to Toth and Aszodi studies [16, 17]. The final number of meshes is about 7400000.

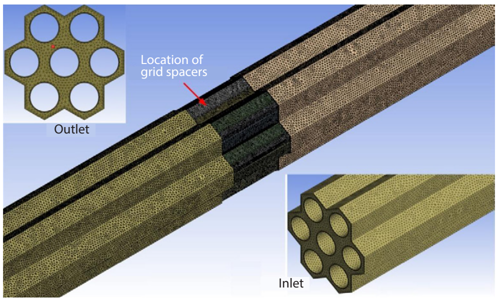

Figure 3. The grid distribution

The standard k-ε model, proposed by Launder and Spalding [32], was used in Ansys-CFX simulation. It is assumed that rod and wall surfaces are smooth for the flow calculations. The heat flux is 278.7 kW/m^2 on the surface of the rods corresponding to the average axial heat flux in modelling of the domain in the VVER-1000 reactor at full power [15]. The water inlet velocity and temperature were 5.6 m/s and 564.15 K, respectively. The equivalent hydraulic diameter was used as the characteristic length in calculating the Reynolds and Nusselt numbers. The Reynolds number for this inlet velocity was 2.3×10^5, well in the turbulent flow regime. The temperature dependent thermophysical properties of the coolant were taken into account which are implemented in the ANSYS CFX 15. The computations were performed in steady-state mode. The fluid flows upward in the rod bundle. The analysis was performed using the commercial CFD code ANSYS CFX 15. The convergence criteria were 10^{-6} for the root mean square of equation residuals and 0.01% for the imbalances, respectively.

Results and discussion

Velocity and flow mixing parameters

Figure 4 shows the variation of velocity magnitude of coolant over the centerline of the central subchannel. As depicted in fig. 4, the velocity magnitude is shaped over the grid spacer and mixing vanes. To show the development of the swirling flow in the subchannel velocity vectors upstream and downstream of spacer grid at six axial (z-direction) locations are shown in fig. 5. It is surprising that as the flow develops

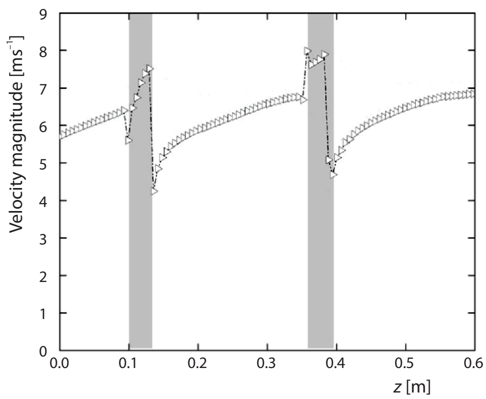

Figure 4. Velocity magnitude of coolant along the central subchannel

in the axial direction, the swirling flow in subhchanel with mixing vane generate the swirling flow in the subchannel without mixing vanes. A possible explanation for this might be that as the flow develops in the axial direction, the swirling flow does not remain in the center of the subchannel and there is a strong outflow in the rod gap which could generate a swirl flow in the subchannel without mixing vane.

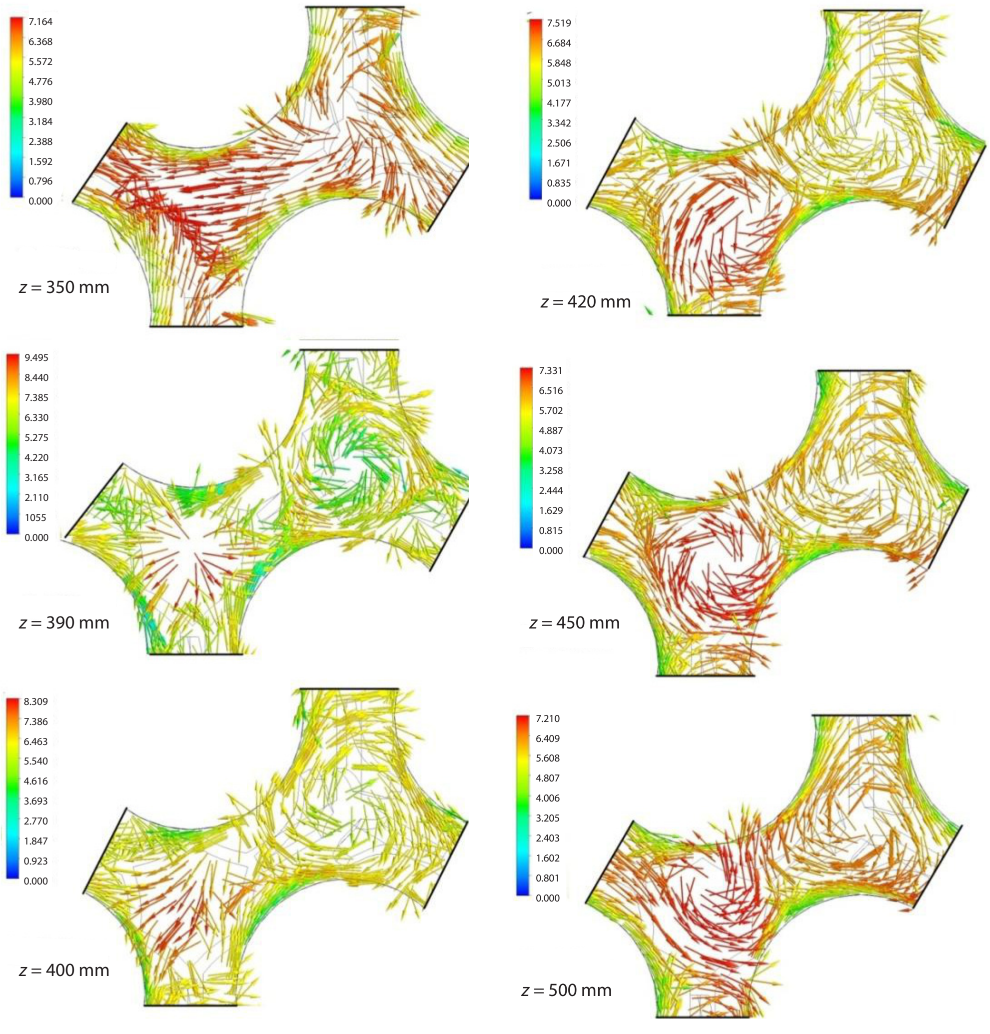

Figure 5. Velocity vectors downstream and upstream of spacer at different location

Temperature distribution and heat transfer

For engineering safety design purposes the key issue is to know the temperature distribution of coolant and fuel rod cladding surface for normal and abnormal conditions. Figure 6 illustrates the mass-averaged cross-sectional temperature along the rod bundle. Note that there has been a steady increase in the coolant temperature distribution along the rod bundle for all the cases. As the coolant moves along the rod bundle, it absorbs heat. As a result, its temperature continues to rise. The coolant temperature increases steadily in the central subchannel, whereas it dips passing each grid spacer in the channel with spacers. Figure 7 shows the wall heat transfer coefficient along the central fuel bundle. Note that the heat transfer coefficient shoots up at the location of mixing vanes and then reaches a fully developed value further downstream of the each grid spacer where the flow already reached hydrodynamically developed condition. This peaking is attributed to turbulence increase at the location of mixing vane. Beyond the maximum point, the heat transfer coefficient decreases gradually towards the end of the bundle grid spacers and hits the bottom. A possible explanation for this might be that the decreased flow area due to grid spacer and mixing vanes accelerates the fluid-flow and results in higher fluid velocities at the location of spacer grid and downstream of the grid which boost the local heat transfer.

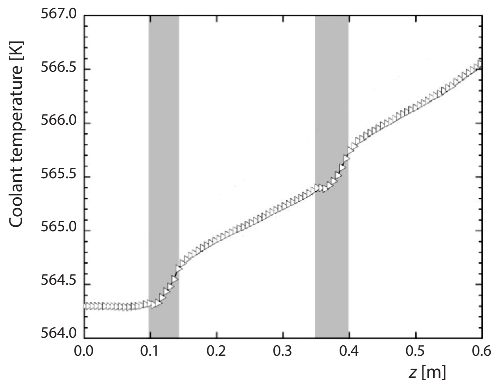

Figure 6. Coolant temperature [$T_b(z)$] along the central subchannel [K]

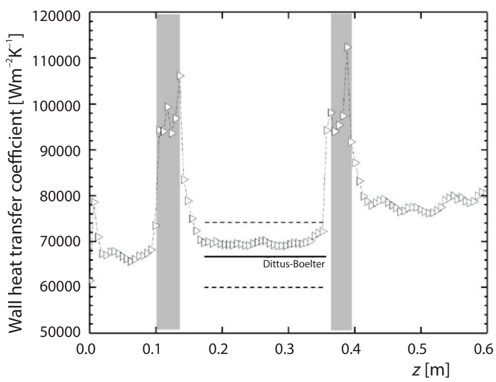

Figure 7. Wall heat transfer coefficient [$Wm^{-2}K^{-1}$]

The local Nusselt number, Nu(z), is calculated according to the expression (1). The local convective heat transfer coefficient $h(z)$ in experession (1) is defined as expression (2).

$$\mathrm{Nu}(z) = \frac{h(z) D_h}{k} \tag{1}$$

$$h(z) = \frac{q''}{T_\mathrm{w}(z) - T_\mathrm{b}(z)} \tag{2}$$

In order to validate the heat transfer coefficient of this study, the Dittus-Boelter equation for turbulent flow has been used to validate the fully developed heat transfer coefficients in the rod bundles, eq. (3). Morover the normalized Nusselt number, $\mathrm{Nu}(z)/\mathrm{Nu}_\infty$, in between the two spacer grids is compared with the correlation proposed by Yao *et al*. [5]. is the fully developed Nusselt number downstream of the first grid spacer. The thermal conductivity of water, k, was calculated at the local bulk mean temperatures. Yao *et al*. [5] proposed a correlation (3) based on heat transfer measurements from rod bundles with spacer grids in an experimental test facility with gas coolant. Note that correlation (3) is applicable for Reynolds number higher than 104.

$$\mathrm{Nu}_\infty = 0.023\mathrm{Re}^{0.8}\mathrm{Pr}^{0.4} \tag{3}$$

$$\frac{\mathrm{Nu}(z)}{\mathrm{Nu}_\infty} = 1 + 5.55\varepsilon^2 \exp\left(-0.13\frac{z}{D_h}\right) \tag{4}$$

Figure 8 show the variation in in between the two spacer grids. According to the fig. 8, the region downstream of the grid spacer can be divided into two parts. The first part, from

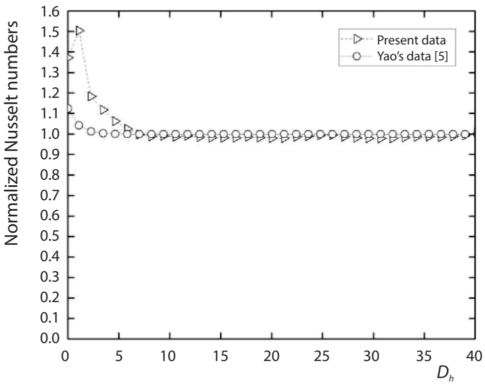

Figure 8. Developments of normalized Nusselt numbers

z/D_h = 0 to approximately z/D_h = 10, is the effective region. The second part is beyond z/D_h = 10 where the flow is fully developed. The local Nusselt number along z-direction has a maximum value at the location of the first grid spacer and then exponentially decays to the fully developed value downstream of the grid spacer up to about z/D_h = 10. The deviation of CFD data with the of Yao's correlation is probably due to the difference in the experimental conditions and working fluid.

The temperature contours colored by velocity vectors are shown in fig. 9 on particular x-y planes along the computational domain. The variation in velocity is also shown in the middle. The split mixing vane creates a circle shape vortex with a clockwise rotation. The mixing vane creates strong lateral flow through the rod gaps which promotes fluid exchange and flow mixing between neighboring subchannels. As the flow progresses downstream of the mixing vanes, the swirl flow structure decreases and the vortex becomes more circular in shape which could cause considerable convective mixing between the adjoining subchannels. The velocity associated with the swirl flow in the subchannel is significantly higher than that in the rod gaps. Surprisingly, as the flow develops in the axial direction, the swirl flow in subchannel with mixing vane is generated in the subchannel without mixing vanes as well. A possible explanation for this might be that as the flow develops in the axial direction, the swirl flow does not remain in the center of the subchannel and there

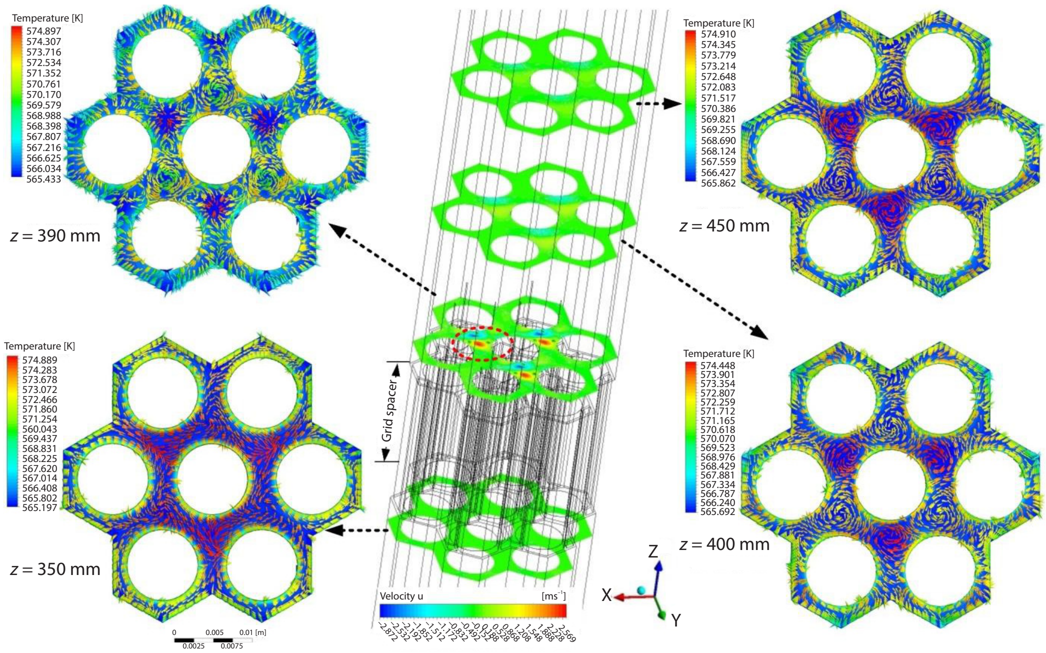

Figure 9. Contour of temperature colored by velocity vectors at different planes along the computational domain

is a strong outflow in the rod gap which could generate a swirl flow in the subchannel without mixing vane. This study confirms that the attachment of mixing vanes increase thermal performance by promoting the turbulence level, increasing inter-subchannel mixing, and inducing swirl flow in the subchannels. The circumferential variation in the average wall heat transfer coefficient for the central rod is depicted fig. 10. The heat transfer coefficient is higher at the location close to the vanes corresponding to $\theta = 60°$, 180°, and 300°.

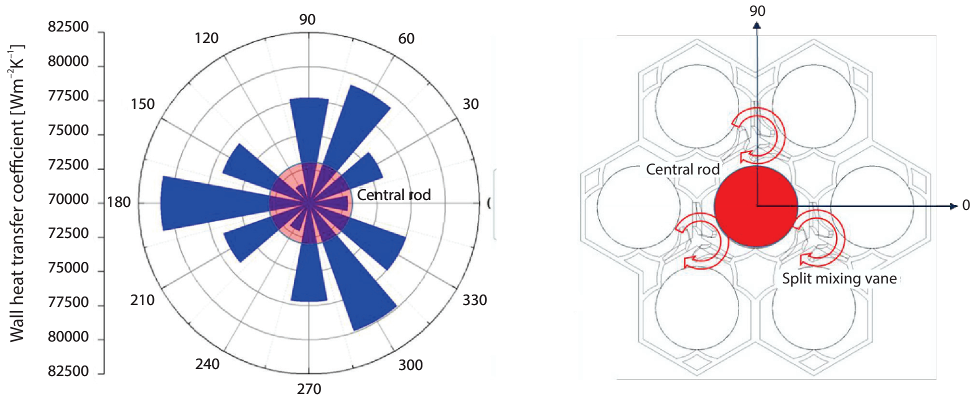

Figure 10. Circumferential variation of averaged wall heat transfer coefficient for central rod

Pressure drop calculation

One of the important parameter in designing the VVER fuel bundle is the pressure drop because it significantly influences the pressure loss of the reactor core, therefore, the required pumping power. Hence it is important to predict accurately the pressure drop of the fuel bundle. Figure 11 illustrates the variation of the mean pressure in sub-channels along the z direction. From z = 100-130 mm, where the spacer grid is located, the pressure drops rapidly due to the local hydraulic resistance of the spacer grid. This result may be explained by the fact that the presence of the spacer grid reduces the flow cross-sectional area, increases the fluid velocity between the grid straps and rods, and results in extra wall frictional resistance of straps [31]. Between 130 mm and 135 mm where the split mixing vane is located, the pressure suddenly decreases due to local resistance of mixing vane. In the downstream of mixing vane grid spacer grid, at first the pressure shoots up because the cross-sectional area in the subchannel becomes large, then declines gradually due to frictional drag. In other words, there is a clear trend of increasing pressure drop passing the mixing vane grid spacers due to the flow area contraction. The overall static pressure drop along the computational domain consists of the friction losses in bare rod bundle and local losses at the location of grid spacers and mixing vane. For a bare rod bundle the friction pressure loss can be calculated from the Darcy-Weisbach formula, eq. (1).

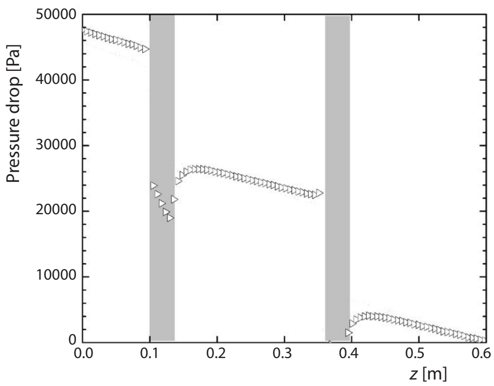

Figure 11. Pressure drop along the rod bundle

$$\frac{\Delta P}{\Delta z} = \lambda \frac{1}{D_h} \frac{1}{2} \rho V^2 \tag{5}$$

There is a large volume of published studies [1-3, 7-9, 12-18, 31] evaluating the pressure loss due to presence of grid spacers in rod bundle. Rehme [1-3] in systematic experimental studies, showed that the pressure loss across spacer grids is mainly due to the blockage of the flow area and the pressure loss coefficient of the spacer grids. He proposed the following correlations for the total pressure drop due to all of the grid spacers. The spacer designs considered in Rehme's studies [1-3] were of honeycomb-type (triangular and square array), triangular-type, rhombus type, spacer coils, tube spacers (axially and transversally connected) and ring-type [15].

$$\Delta P_{GS} = \frac{1}{2} N_{GS} C \varepsilon^2 V^2 \tag{6}$$

Cigarini and Donne [7] have experimentaly developed a model to predict the spacer loss coefficient based on Rehme's model, and proposed a modified drag coefficient eq. (7).

$$C_{C,D} = \min\left[\left(3.5 + \frac{73.14}{\mathrm{Re}^{0.264}} + \frac{2.79 \cdot 10^{10}}{\mathrm{Re}^{2.79}}\right) \text{ or } \frac{2}{\varepsilon^2}\right] \tag{7}$$

where ε ranges from 0.15-0.4 for typical grid spacer designs [14]. The pressure drop calculation using the equation is presented in tab. 1. The pressure loss due to presence of grid spacer is in a reasonable range compared with Rehme's data [1]. A similar approach with Wu *et al.* [31] was chosen to specify the pressure loss of split mixing vane in this study. The pressure loss due to split mixing vane is approximately 2.1 KPa.

Table 1. Pressure drop calculation [KPa]

	Numerical calculation	Experimental correlation [7]
Grid spacer	15.1	16.8
Grid spacer and mixing vane	17.15	–
Total pressure drop	47.65	44.85

Conclusion

The purpose of the current study was mainly to simulate the flow dynamics for VVER type reactors using the CFD tools. Numerical study has been presented of the axial development of swirl flow in a VVER type rod bundle subchannel. Swirl flow was introduced in the subchannel from the split mixing vane located on the downstream edge of the VVER support grid. The most obvious finding to emerge from this CFD study is that regarding manufacturing possibilities, split mixing vane significantly enhances the local heat transfer for a VVER fuel assembly subchannel. As the flow is developed in the axial direction passing the mixing vanes, the swirl flow migrates away from the center of the subchannel and generates swirl flow in other subchannels without mixing vane. These findings could be beneficial for next generation of VVER such as VVER-1200. The coupled thermohydrodynamics and neutronics would indeed constitute more rigorous analyses of the mixing vane design for next generation of PWR.

Acknowledgment

The authors appreciate Energy Research Institute of University of Kashan for support of this work.

Nomenclature

D_h – equivalent hydraulic diameter, [m]
h – heat transfer coefficient, [Wm^{-2} K^{-1}]
k – thermal conductivity, [Wm^{-1}K^{-1}]
N_{GS} – number of grid spacers in a fuel assembly
Nu – Nusselt number
P – pressure, [Pa]
Pr – Prandtl number
q'' – heat flux, [Wm^{-2}]
Re – Reynolds number
T – temperature, [K]
u, v – velocity component, [ms^{-1}]
x, y, z – spatial co-ordinates, [m]
V – mean velocity (Re averaged)

Greek symbols

ε – subchannel blockage factor
ρ – density, [kgm^{-3}]
λ – friction factor

Subscript

b – bulk
w – wall
∞ – value at fully developed region

References

[1] Rehme, K., Pressure Drop Correlations for Fuel Element Spacers, *Nuclear Technology*, *17* (1973), 1, pp. 15-23
[2] Rehme, K., Pressure Drop of Spacer Grids in Smooth and Roughened Rod Bundles, *Nuclear Technology*, *33* (1977), 3, pp. 314-317
[3] Rehme, K., Trippe, G., Pressure Drop and Velocity Distribution in Rod Bundles with Spacer Grids, *Nuclear Engineering and Design*, *62* (1980), 1-3, pp. 349-359
[4] Bragina, V. L., *et al*., Experimental Study of Enhancement of Heat Transfer From a Tube Bundle in Turbulent Axial Flow, Heat transfer, *Soviet research*, *13* (1981), 4, pp. 14-18
[5] Yao, S. C., *et a*l., Heat Transfer Augmentation in Rod Bundle Near Grid Spacers, *Journal of Heat Transfer*, *104* (1982), 1, pp. 76-81
[6] Chesna, B. A., Kolesnikovas, I. Y., Influence of Spacer Grids on the Rate of Heat Transfer in an Air Stream Flowing Longitudinally Through a Bundle of Rods, *International Chemical Engineering*, *27* (1987), 1, pp. 158-161
[7] Cigarini, M., Donne, D. M., Thermohydraulic Optimization of Homogeneous and Heterogeneous Advanced Pressurized Reactors, *Nuclear Technology*, *80* (1988), 1, pp. 107-132
[8] In, W. K., *et al.*, Flow Analysis for Optimum Design of Mixing Vane in a PWR Fuel Assembly, *Journal of the Korean Nuclear Society*, *33* (2001), 3, 327
[9] Kim, K. Y., Seo, J. W., Shape Optimization of a Mixing Vane in Subchannel of Nuclear Reactor, *Journal of Nuclear Science and Technology*, *41* (2004), 5, pp. 641-644
[10] Ikeda, K., *et al*., Single-Phase CFD Applicability for Estimating Fluid Hot-Spot Locations in a 5 × 5 Fuel Rod Bundle, *Nuclear Engeering Design*, *236* (2006), 11, pp. 1149-1154
[11] Ikeno, T., *et al*., The Effect of Mixing Vane Arrangements in a Subchannel Turbulent Flow, *Journal of Nuclear Science and Technology, 43* (2006), 10, pp. 1194-1205
[12] Song, K. N., *et al.*, Performance Evaluation of New Spacer Grid Shapes for PWR, *Journal of the Korean Nuclear Society*, *39* (2007), 6, pp. 737-347
[13] Nematollahi, M. R., Nazifi, M., Enhancement of Heat Transfer in a Typical Pressurized Water Reactor by Different Mixing Vanes on Spacer Grids, *Energy Conversion Management*, *49* (2008), 7, pp. 1981-1988
[14] Schikorr M., *et al.*, Proposal for Pressure Drop Prediction for a Fuel Bundle with Grid Spacers using Rehme Pressure Drop Correlations, *Nuclear Engineering Design*, *240* (2010), 7, pp. 1830-1842
[15] Ganjiani, H., Firoozabadi, B., The 3-D Simulation of Turbulent Flow in 3-sub Channels of a VVER-1000 Reactor, *Sharif University of Technology Transaction B: Mechanical Engineering*, *17* (2010), 2, pp. 83-92
[16] Toth, S., Aszodi, A., The CFD Analysis of Flow Field in a Triangular Rod Bundle, *Nuclear Engineering Design*, *240* (2010), 2, pp. 352-363
[17] Toth, S., Aszodi, A., The CFD Study on Coolant Mixing in VVER-440 Fuel Rod Bundles and Fuel Assembly Heads, *Nuclear Engineering Design*, *240* (2010), 9, pp. 2194-2205
[18] Navarro, M. A., Santos, A. C., Evaluation of a Numeric Procedure for Flow Simulation of a 5 × 5 PWR Rod Bundle with a Mixing Vane Spacer, *Progress of Nuclear Energy*, *53* (2011), 8, pp. 1190-1196
[19] Sang-Ki, M., *et al.*, Single-phase Convective Heat Transfer Enhancement by Spacer Grids in a Rod Bundle, *Journal of Nuclear Science and Technology*, *51* (2014), 4, pp. 543-557

[20] Chang, S. K., *et al.*, Turbulent Mixing in a Rod Bundle with Vaned Spacer Grids: OECD/NEA–KAERI CFD Benchmark Exercise Test, *Nuclear Engineering and Design*, *279* (2014), Nov., pp. 19-36
[21] Lee, J. R., *et al.*, Synthesis of the Turbulent Mixing in a Rod Bundle with Vaned Spacer Grids Based on the OECD-KAERI CFD Benchmark Exercise, *Nuclear Engineering and Design*, *279* (2014), Nov., pp. 3-18
[22] Cinosi, N., *et al.*, The CFD Simulation of Turbulent Flow in a Rod Bundle with Spacer Grids (MATIS-H) using STAR-CCM+, *Nuclear Engineering and Design*, *279* (2014), Nov., pp. 37-49
[23] Bieder, U., *et al*., The LES Analysis of the Flow in a Simplified PWR Assembly with Mixing Grid, *Progress in Nuclear Energy*, *75* (2014), Aug., pp. 15-24
[24] In, W. K., *et al.*, Measurement and CFD Calculation of Spacer Loss Coefficient for a Tight-Lattice Fuel Bundle, *Nuclear Engineering and Design*, *284* (2015), Apr., pp. 153-161
[25] Lee, *et al*., Augmentation of Single-phase Forced Convection Heat Transfer in Tightly Arrayed Rod Bundle with Twist-Vane Spacer Grid, *Experimental Thermal and Fluid Science*, *76* (2016), Sept., pp. 185-192
[26] Hutli, E., *et al*., Experimental Approach to Investigate the Dynamics of Mixing Coolant Flow in Complex Geometry using PIV and PLIF Techniques, *Thermal Science*, *19* (2015), 3, pp. 989-1004
[27] Qin, S., *et al.*, Experimental Investigation on Repeatability of CHF in Rod bundle with Non-Uniform Axial Heat Flux Distribution, *Progress in Nuclear Energy*, *90* (2016), July, pp. 151-154
[28] Mao, H., *et al*., Modelling of Spacer Grid Mixing Effects through Mixing Vane Crossflow Model in Subchannel Analysis, *Nuclear Engineering and Design*, *320* (2017), Aug., pp. 141-152
[29] Chen, X., *et al*., Validation of CFD Analysis for Rod Bundle Flow Test with Vaned Spacer Grids., *Annals of Nuclear Energy*, *109* (2017), Nov., pp. 370-379
[30] Shashi Kant, V., *et al*., Experimental Investigation of Effect of Spacer on Single Phase Turbulent Mixing Rate on Simulated Subchannel of Advanced Heavy Water Reactor, *Annals of Nuclear Energy*, *110* (2017), Dec., pp. 186-195
[31] Wu, J. M., *et al*., The CFD Analysis of the Impact of a Novel Spacer Grid with Longitudinal Vortex Generators on the Sub-Channel Flow and Heat Transfer of a Rod Bundle, *Nuclear Engineering and Design*, *324* (2017), Dec., pp. 78-92
[32] Launder, B. E., Spalding, D. B., The Numerical Computation of Turbulent Flows, *Computer Methods in Applied Mechanics and Engineering*, *3* (1974), 2, pp. 269-289

Paper submitted: October 6, 2017
Paper revised: January 31, 2018
Paper accepted: February 3, 2018